

Wintertime mapping and monitoring of sea ice temperatures surrounding Antarctica using SSM/I data

T. J. Majumdar* and S. Bhattacharya

Space Applications Centre (ISRO), Ahmedabad – 380 015, India

*Corresponding author: E-mail: tjmajumdar@rediffmail.com

ABSTRACT

The Polar Regions are known to be highly sensitive to warming effects of the increased greenhouse gases. Sea ice, together with land ice, exerts profound influence in controlling the global climate. Mapping and monitoring of sea ice concentration and sea ice temperature around Antarctica during wintertime have been attempted here with NASA Team Algorithm. Results obtained concur well with those obtained by other workers. Major sea ice concentrations vary between 80-100% during August 2002 with more number of classes and sea ice temperatures are found in the range of 230 to 250 K.

INTRODUCTION

Antarctica, the fifth largest continent on the Earth (area approximately 14 million square kilometers), is almost totally (around 98%) covered by ice, which accounts for almost 4.5% of the earth's surface area. It is also the coldest continent with ambient air temperature varying from -80°C to -30°C throughout the year. It contains huge reserves of valuable minerals, coal and petroleum (Antarctica – Wikipedia; Behrendt 1983). About 90% of the world's ice is present over the Antarctic landmass and in its surrounding Southern Ocean, and if melted, would raise the ocean by 60 m (Massom 1991). Massive thickness of ice overlying the Antarctic landmass makes it the highest continent on the earth. Thicknesses of ice at places are beyond 4500 m, the average thickness being approximately 2100 m (Gloersen et al. 1992; Majumdar & Mohanty 2000).

Sea ice being one of the most dynamic and ephemeral geophysical features on the earth's surface exerts a profound influence on local and global climatic and oceanic regimes along with land ice. The ice sheets of both the Polar Regions account for almost 10% of the earth's surface area, and their high albedo and thermal and radiative properties are climatically highly significant. Moreover, polar ice masses, and the ice sheets in particular, are depleting very fast in response to an increase in atmospheric 'greenhouse gases' such as methane and CO_2 , which is caused mainly due to the excessive burning of fossil

fuels in the recent past (Massom 1991).

In polar oceans of both the hemispheres, sea ice forms through the freezing of sea water over large areas and covers as much as 30×10^6 sq km of the earth's surface (Massom 1991). By virtue of its high reflectivity, high latent heat and low thermal conductivity, a sea ice cover greatly modifies – a) ocean mixing processes, b) surface roughness and thus momentum transfer between atmosphere and ocean, c) the vertical and horizontal transfer of heat and moisture between atmosphere and the relatively warm ocean, and d) atmospheric boundary layer structure (Foster & Carmack 1976). These processes depend strongly on the time and location because of the high temporal and spatial variability of the sea ice cover in each hemisphere (Massom 1991; Gloersen et al. 1992). In order to understand the atmosphere-ocean interactions and exchanges of heat, mass and momentum, and their influences on the ocean and climate variability from the local to global scale and the biological productivity of the ice and ocean, a thorough knowledge of the spatial and temporal variation in the Antarctic sea ice cover as well as sea ice temperature is essential (Jeffries et al. 1998; Sreenivasan & Majumdar 2006).

The study of spatial as well as temporal variations in the sea ice cover and sea ice temperature is thus of prime importance in understanding atmosphere-ocean interactions and for studying other climate and oceanography related parameters. A recent survey by National Snow and Ice Data Center (NSIDC),

Colorado using MODIS data reveals that around 13,680 sq km ice shelf (e.g. Wilkins Ice Shelf, Larsen B Ice Shelf, Ross Ice Shelf etc.) has begun collapsing due to change in a fast warming region of Antarctica (NSIDC Notes 2008). For the reasons cited above, the present study of derivation of sea ice temperature in the Southern Ocean surrounding Antarctica using SSM/I passive microwave data has been attempted.

Passive Microwave Remote Sensing

The advantage of the passive microwave sensors over optical and infrared scanners lies in the fact that they remain unaffected by cloud cover. They can acquire data at nighttime as well since they record emitted radiation rather than reflected solar radiation. Thus passive microwave radiometers give a synoptic coverage of the earth's surface (Cracknell & Hayes 2000). However, passive microwave sensors operating at microwave wavelengths ($\sim 6\text{-}90$ GHz) have almost no effect on dense ice packs and thus can easily penetrate through ice covers (Ulaby et al. 1986). Since the emissivity of an object depends very much on its composition and physical structure, hence, important information on emissivity and physical properties and conditions of the emitting medium can be derived from measurements of TB from space (Zwally et al. 1983; Massom 1991).

The equation $\varepsilon = T_B/T_S$ (where ε is the emissivity, T_B is the brightness temperature of the object in degrees Kelvin and T_S is the physical temperature of the object in degrees Kelvin) holds good only in case of emissions coming out of an isothermal medium. Since the natural media are not isothermal, therefore, a radiative transfer function describing the transfer of radiation from a given point within the medium to the surface is used as a weighting function to obtain the effective physical temperature. Variation in the values of emissivity with wavelength and polarization makes it possible to obtain the physical properties of a medium from radiometric measurements of T_B using multiple frequencies and dual polarization. Hence multichannel microwave sensors are found to be more useful than the single channel. Vertically (V) polarized T_B are greater than those measured at horizontal (H) polarization. The contrast between open water and sea ice is greater with H polarization and increases with increasing wavelength (Massom 1991). The large contrast between microwave

emissivities of open water (around 0.4 at 10 GHz) and sea ice (0.7-0.9) makes it possible to delineate ice edges and estimate the concentrations of sea ice of the polar oceans using passive microwave sensors (Gloersen et al. 1973; Massom 1991).

OBJECTIVES

Major objective of this study is to derive the sea ice concentrations and temperatures from SSM/I passive microwave brightness temperature data over the Southern Ocean surrounding the Antarctic continent during the major period of sea ice accumulation (April to September, 2002), using existing algorithms and to study the spatial and temporal variation in sea ice temperature and the probable reason behind such variation.

STUDY AREA AND DATA USED

The present study has been carried out over the Antarctic continent and the surrounding Southern Ocean (Fig. 1a) which is divided into five sectors (Fig. 1b). We used data from the Special Sensor Microwave Imager (SSM/I), which is a seven-channel, four frequencies linearly polarized passive microwave radiometer system on-board DMSP-F8, DMSP-F11 and DMSP-F13 satellites launched under the Defense Meteorological Satellite Program (DMSP), USA. The instrument measures combined atmosphere and surface radiances at 19.35, 22.235, 37.0 and 85.5 GHz frequencies. Vertical and horizontal polarizations are available for each frequency except the 22.235 GHz channel, which has vertical polarization only (NSIDC Reports 1999; Maslanik & Stroeve 2002). For the study of the sea ice and glaciers over Antarctica, the DMSP Special Sensor Microwave Imager (SSM/I) passive microwave data from April to September, 2002 have been used with 19 GHz H and V and 37 GHz V channels due to their sensitivity to snow/ice mapping/monitoring. Spatial resolution of SSM/I is around 25 km for 19.35, 22.235, 37.0 GHz channels and 12 km for 85.5 GHz channel. Results obtained in this study were compared with those obtained by Comiso et al. (2003) using Advanced Microwave Scanning Radiometer-EOS (AMSR-E) passive microwave data with 6 channels namely, 6.9, 10.7, 18.7, 23.8, 36.5, 89.0 GHz with grid resolution approx. 25 km. In addition, NOAA AVHRR (Advanced Very High

Wintertime mapping and monitoring of sea ice temperatures surrounding Antarctica using SSM/I data

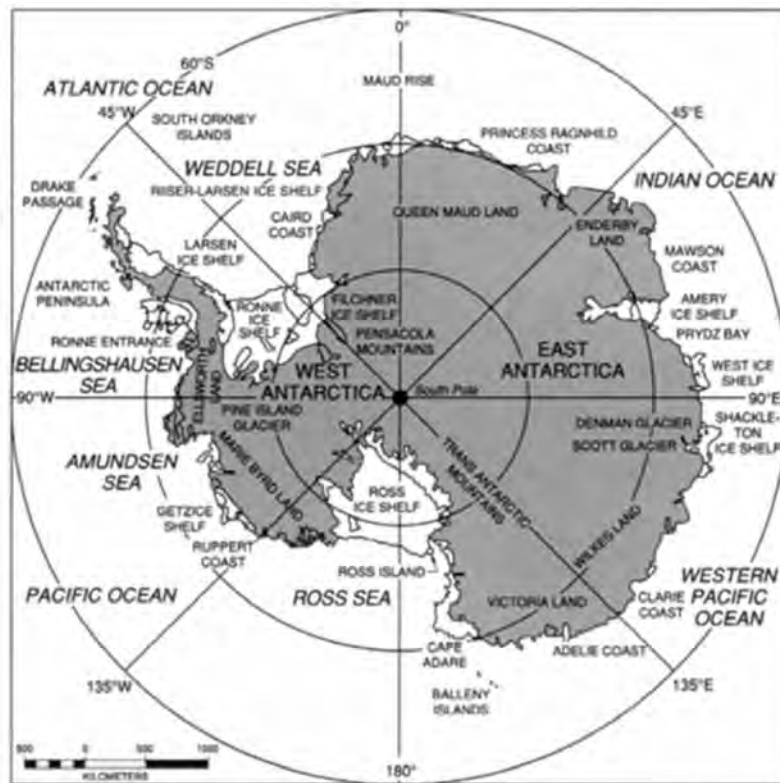


Figure 1a: Antarctic Location Map (after Gloersen et al. 1992)

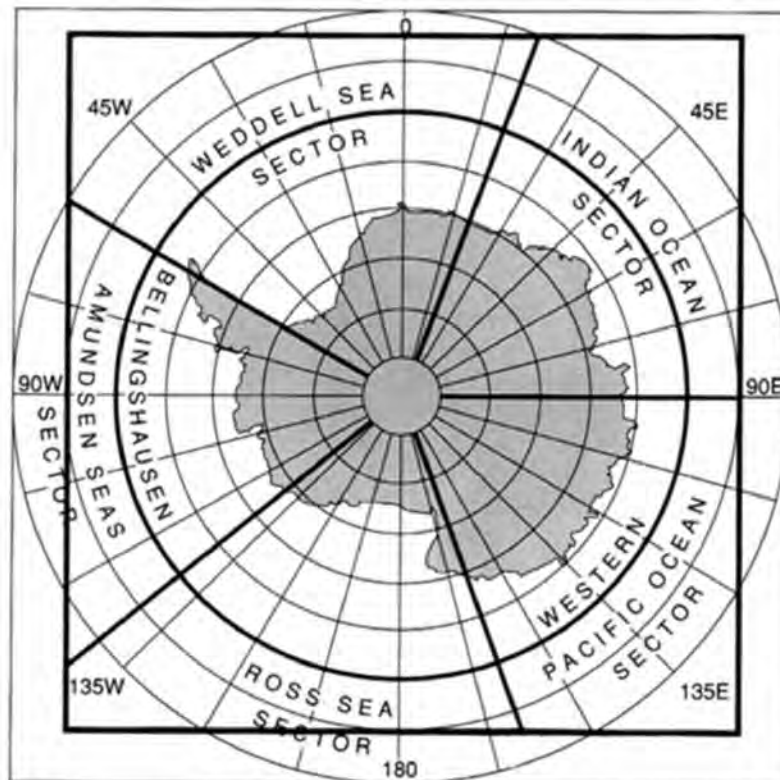


Figure 1b: Antarctic Sector Map (after Gloersen et al. 1992)

Resolution Radiometer) data with five channels and spatial resolution ~ 1 km have been used for sea surface skin temperature estimation mainly with channel 4 (10.3-11.3 μm) and channel 5 (11.5-12.5 μm) in cloud-free conditions.

METHODOLOGY

Derivation of Sea Ice Concentration (NASA Team Algorithm)

The NASA Team Algorithm makes use of both frequency and polarization information at 19 and 37 GHz (Cavalieri et al. 1984; Burns 1993). Determination of sea ice concentration is based on the fact that at 19 GHz, both horizontal and vertical polarizations of open water are much greater than that of ice (Burns 1993). Also, the difference between the vertical and horizontal brightness temperatures is consistently greater (i.e., more polarized) for open water than for either ice type at all wavelengths. A polarization ratio (PR) is defined as:-

$$PR = (T_{B(19V)} - T_{B(19H)}) / (T_{B(19V)} + T_{B(19H)}) \quad \dots (1)$$

The relationship between 19 and 37 GHz is used to resolve the variations in ice signatures from ice-concentration variations. Accordingly, a spectral gradient ratio is defined as:-

$$GR = (T_{B(37V)} - T_{B(19V)}) / (T_{B(37V)} + T_{B(19V)}) \quad \dots (2)$$

The total ice concentration is given as:-

$$C = (A_0 + A_1 * PR + A_2 * GR + A_3 * PR * GR) / (B_0 + B_1 * PR + B_2 * GR + B_3 * PR * GR) \quad \dots (3)$$

where the A s and B s are functions of fixed tie points for ice and open water (Burns 1993).

Derivation of Sea Ice Temperature

Sea ice temperatures are calculated from a single channel of microwave radiation, either 19.35 GHz (V) or 37 GHz (V) brightness temperatures, and the sea ice concentrations. In the present study, 19 GHz (V) channel is used together with already derived sea ice concentrations. The algorithm is as follows (NSIDC Reports 1999):

$$T(f) = [T_B(f) - (1 - C_F - C_M) * \epsilon_{(OW,f)} * T_{OW}] / [C_F * \epsilon_{(F,f)} + C_M * \epsilon_{(M,f)}] \quad \dots (4)$$

where, C_F and C_M are the concentrations of first-year ice and multi-year ice respectively derived from NASA Team Algorithm, F denotes first-year ice, M denotes multi-year ice, f is the given frequency (19V or 37V), ϵ is the emissivity (given for surface type at given frequency), T_{OW} is equal to 271.2K, $\epsilon_{(OW,19V)}$ is equal to 0.57, and $\epsilon_{(OW,37V)}$ is equal to 0.66. NASA Team Algorithm has been discussed in details elsewhere (Cavalieri et al. 1984; 1991).

The emissivities for ice were empirically derived from comparisons with AVHRR skin temperature and are considered 'effective emissivities' for deriving temperature, not necessarily true emissivities. First year (FY) and Multi-year (MY) sea ice during winter can be calculated using different algorithms as given in the earlier studies (Gloersen et al. 1992; Maslanik & Key 1993; Comiso et al. 2003).

Physical Temperature Retrieval from AVHRR

Snow/ice temperatures as estimated from both AVHRR and passive microwave data are functions of physical temperature, emissivity, ice concentration and ice thickness. Penetration depth in snow/ice column increases as microwave frequency decreases. Thus, the microwave temperatures represent the physical temperature and emissivity at different depths in the ice pack (including snow on the ice surface), whereas the AVHRR-derived values represent surface or very-near-surface temperatures (Maslanik & Key 1993). For the retrieval of snow/ice surface temperature, a multi-channel algorithm that uses the split-window channel computation technique for removal of water-vapor effects, has been utilized (Key & Haefliger 1992; Maslanik & Key 1993).

This involves the differencing of two spectrally adjacent channels with different responses to atmospheric effects e.g. channel 4 (10.3-11.3 μm) and channel 5 (11.5-12.5 μm) of the AVHRR (Key & Haefliger 1992):

$$T_{B(AVHRR)} = a + bT_4 + cT_5 + d[(T_4 - T_5)] \sec \theta \quad \dots (5)$$

where a , b , c and d are empirically derived constants. T_4 and T_5 are the satellite-measured brightness temperatures (K) in the AVHRR thermal channels

Wintertime mapping and monitoring of sea ice temperatures surrounding Antarctica using SSM/I data

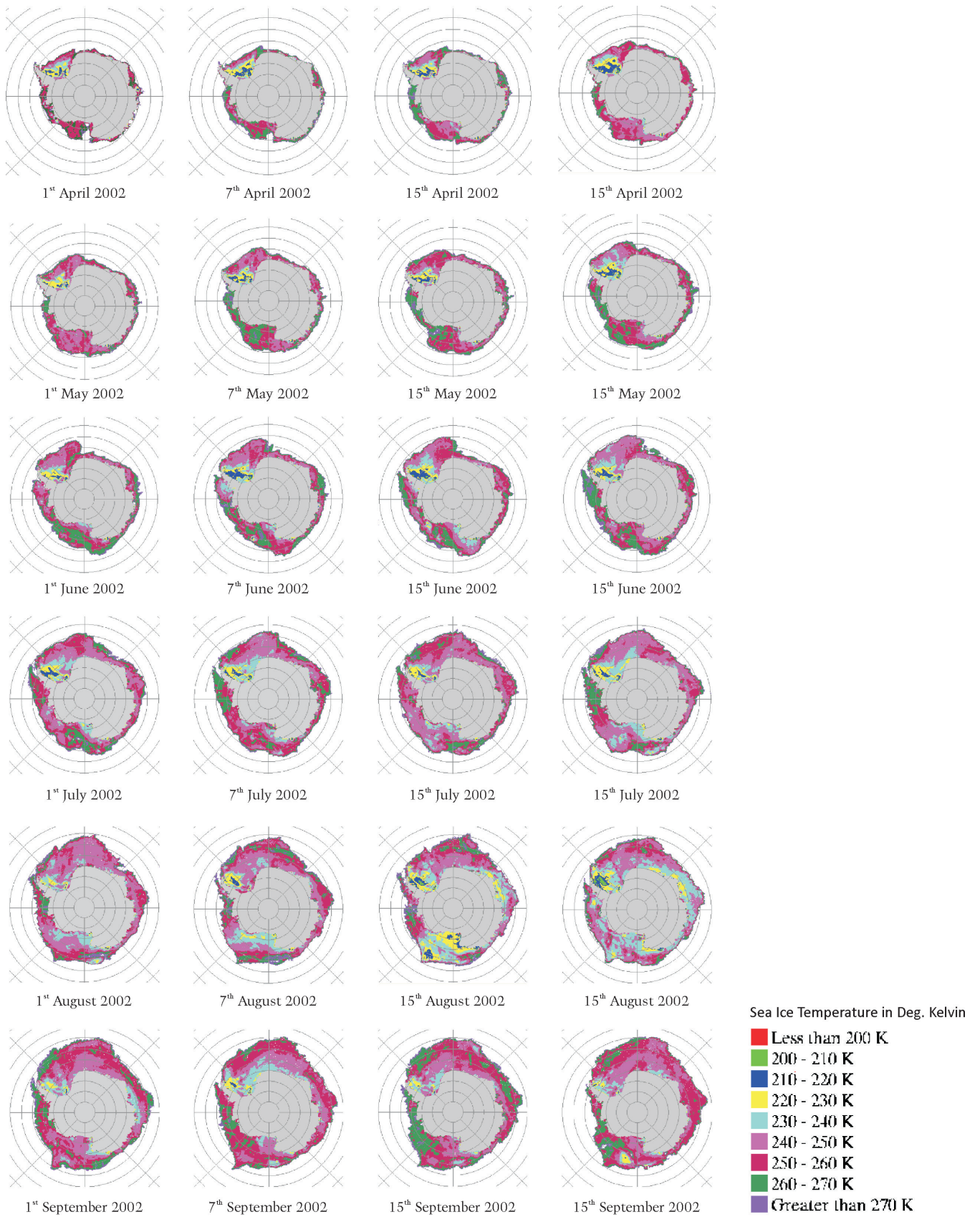


Figure 2: Sea ice temperature maps during April-Sept., 2002 generated using SSM/I data

and θ is the sensor scan angle. This temperature is utilized to estimate the temperature on the interface of snow and ice, which is the radiating layer. Now, passive sensors estimate the brightness temperature (T_B) values, which is a product of surface emissivity and physical temperature, over the sea surface. In general, the microwave-derived sea ice temperatures are lower than the corresponding AVHRR temperatures; with the difference increasing as ice temperature decreases. Since lower ice temperatures are typically associated with a greater percentage of multi-year ice, this difference may be due to an overestimate of multi-year ice emissivity (Maslanik & Key 1993).

RESULTS AND DISCUSSION

Spatial and Temporal Variations in Sea Ice Temperatures over Antarctica

Sea ice temperatures over the Southern Ocean surrounding the Antarctic continent have been derived for the period of April to September, 2002 for every 1st, 7th, 15th and 23rd day of each month (Fig. 2). On 1st April, sea ice temperature in the Ross Sea Sector ranges from 250-270 K. But the major part of the Ross Sea Sector shows a temperature range of 250-260 K. In the Weddell Sea Sector, the scenario is different. Here the temperature ranges from 210-250 K but a gradational change in temperature is

also seen starting from the periphery. At the periphery, the temperature is in the range of 240 K and as one moves towards the continent, the temperature decreases gradually through 230 K and then to 210 K. From 15th April onwards, temperature ranging from 240-250 K is found only as small patches. On 15th April, the temperature range that dominates the Ross Sea Sector is 240-260 K. During 1st to 15th of May, the sea ice temperature drops down to 215-220 K and less in the parts of Weddell Sea Sector with average temperature ranging from 230-240 K. Changes in the patterns of sea ice concentrations in the Ross and Weddell seas during the month of April may have played an active role in the variation of the associated temperature patterns. On 1st June, the scenario has changed to some extent. Temperature ranges from 210-240 K. 240 K temperature is found almost all along the periphery of the sea ice cover. From 15th June to 23rd September, the sea ice temperature shows a wide range of variation from as low as 200 K to as high as 270 K. 260-270 K temperatures were found as small patches mostly in the Ross Sea Sector and Weddell Sea Sector during September. 210-240 K sea ice temperature category is found in considerable amount starting from 15th June up to 23rd September. Maximum areal extent in the 240-250 K ice temperature category takes place on 1st September. Figure 3 shows the areas of sea ice with different temperatures during the overall time-period (April-September, 2002).

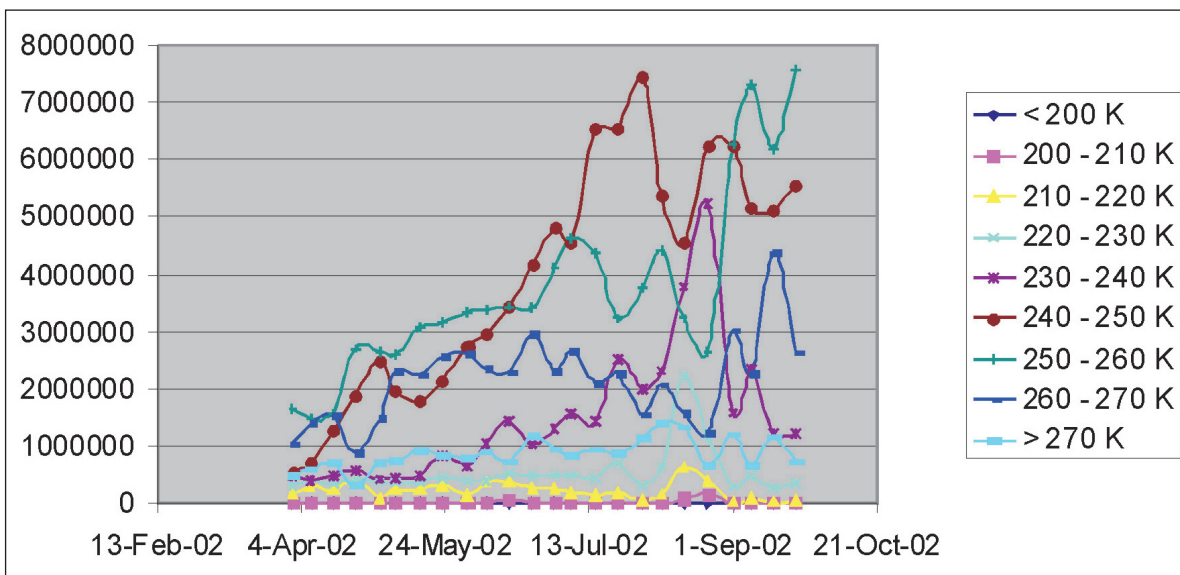


Figure 3: Histogram showing sea ice temperatures during April-Sept., 2002



Figure 4: Sea ice concentration maps during April-Sept., 2002 generated using SSM/I data

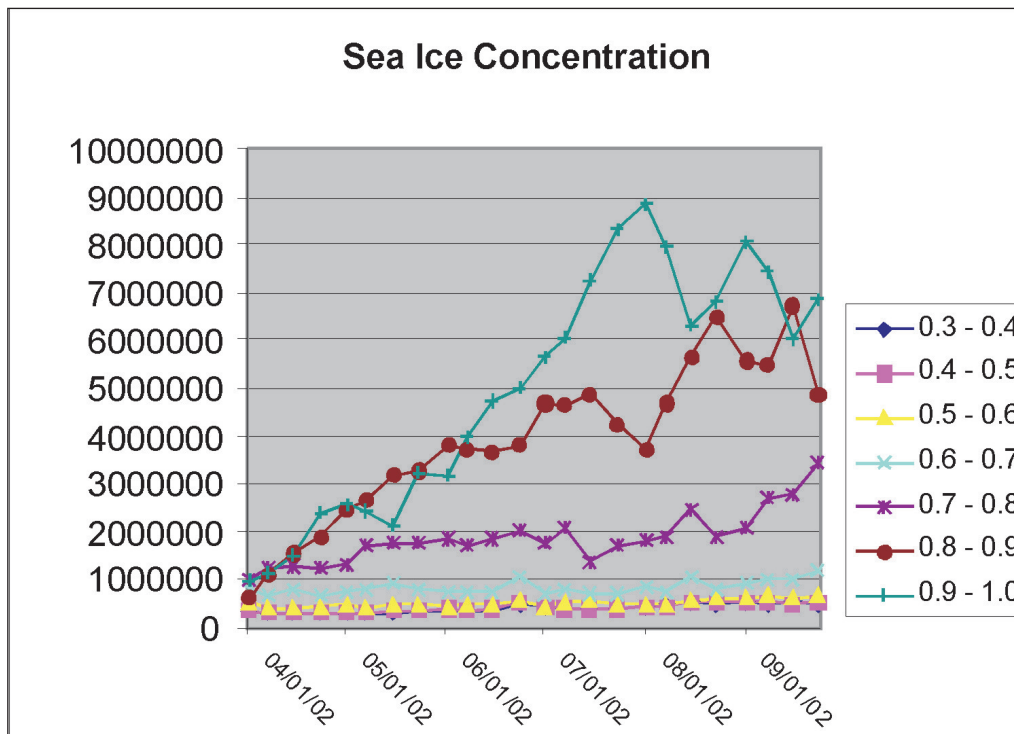


Figure 5: Histogram showing sea ice concentrations during April-Sept., 2002

Sea ice concentration maps also have been plotted for every seven days as shown in Fig. 4. Maximum sea ice concentrations could be observed during August-September. Figure 5 shows the areas of sea ice with different concentrations during the overall time-period (April-September, 2002). Major sea ice concentrations concur well with Comiso et al. (2003) with main concentrations varying between 80-100%, with occurrence of more number of classes during August 2002.

Principal Sources of Errors in Calculating Sea Ice Temperatures

The derived emissivities are the 'effective emissivities' rather than true emissivities as they were empirically derived from comparisons with AVHRR skin temperature. There are errors due to uncertainties in the First-year and Multi-year ice concentration, which can be quite high as ice concentration retrieval goes as an input into the sea ice temperature algorithm. Another major source of error is the presence of any thin ice. Other errors can occur due to snow and other surface effects and the atmospheric effects. The

algorithm is not valid under melt conditions, which generally prevail over Antarctica and its surroundings during the depletion phase (Maslanik & Key 1993; Bhattacharya 2004).

Validation/Comparison of the Results of Sea Ice Temperatures

In the present study, the results obtained (Fig. 2) are compared with the Antarctic sea ice temperatures during August (13-26) 2002 using AMSR-E data as obtained by Comiso et al. (2003) with ranges between 250-268 K, which matches well with our results with ranges between 240-270 K as on Aug. 15th and 23rd, 2002. However, lower range varies by <10 K, though very few pixels have fallen in that category. More variations in sea ice temperatures (3-4 major classes) could be observed within the prescribed range in the present study (Fig. 2) rather than two major classes as observed by Comiso et al. (2003). Similarly, most of the sea ice concentrations derived in the present study concurs well with Comiso et al. (2003) with main concentrations varying between 80-100% during August 2002 (Fig. 4).

CONCLUSIONS

The purpose of the present study is to understand the spatial and temporal variations of Antarctic sea ice temperature. Antarctic sea ice temperature maps have been generated using SSM/I 19 GHz (H and V) and 37 GHz (V) channel for the period of April to September 2002. It is evident from the study that the temperatures in most of the sea ice areas are found in the range of 230 to 250 K. The results obtained from the present study have been compared with those of Comiso et al. (2003) and are found to be in good agreement with the mean monthly Antarctic sea ice temperatures during August. Similarly, major sea ice concentrations are matching well with Comiso et al. (2003) with main concentrations varying between 80-100% during August 2002. The algorithm is valid only under winter conditions over Antarctica. Major sources of errors in calculating the sea ice concentration/temperatures are due to the ambiguity in discrimination of first year ice with the multi-year ice as well as presence of very thin ice. Validation of results could be concentrated only with August 2002 sea ice concentration/temperatures only as available in the literature (Comiso et al. 2003).

As discussed earlier, Wilkins Ice Shelf, Larsen B Ice Shelf, Ross Ice Shelf etc. have begun collapsing due to change in a fast warming region of Antarctica as studied by NSIDC, Colorado (NSIDC Reports 2008) and hence accurate estimation of sea ice temperature will be further useful for assessing the impact of global warming.

ACKNOWLEDGEMENTS

The authors wish to thank Shri A. S. Kirankumar, Director, SAC for his keen interest in this study. TJM wishes to thank CSIR, New Delhi for Emeritus Scientist Fellowship since January 2011. Color versions of few imageries/figures are available at the website: www.igu.in

REFERENCES

Antarctica – Wikipedia, the free encyclopedia. en.wikipedia.org/wiki/Antarctica.
Behrendt, J.C., 1983. Geophysical and geological studies relevant to assessment of the petroleum resources of Antarctica. *Antarctic Earth Science*, pp. 423-428.
Bhattacharya, S., 2004. Mapping of sea ice and

identifications of glaciers in Antarctica using SSM/I and Seasat microwave data. M. Tech. Dissertation, Dept. of Geology and Geophysics, IIT, Kharagpur, April, 2004, 72 p.
Burns, B.A., 1993. Comparison of SSM/I ice-concentration algorithms for the Weddell Sea. *Annals of Glaciol.*, 17, 344-350.
Cavalieri, D.J., Gloerson, P. & Campbell, W., 1984. Determination of sea ice parameters with the NIMBUS-7 SMMR. *J. Geophys. Res.*, 89, D4, 5355-5369.
Cavalieri, D.J., Crawford, J.P., Drinkwater, M.R., Eppler, D.T., Farmer, L.D., Jentz, R.R. & Wackerman, C.C., 1991. Aircraft active and passive microwave validation of sea ice concentration from the Defense Meteorological Satellite Program: Special Sensor Microwave Imager. *J. Geophys. Res.*, 96, 21989-22008.
Comiso, J.C., Cavalieri, D.J. & Markus, T., 2003. Sea ice concentration, ice temperature, and snow depth using AMSR-E data. *IEEE Trans. on Geosc. & Rem. Sens.*, 41, 243-252.
Cracknell, A.P. & Hayes, L.W.B., 2000. *Introduction to Remote Sensing*, Taylor & Francis Publ., London, 293 p.
Foster, T.D. & Carmack, E.C., 1976. Frontal zone mixing and Antarctic bottom water formation in the southern Weddell Sea. *Deep-Sea Res.*, 23, 301-317.
Gloersen, P., Nordberg, W., Schumge, T. & Campbell, W., 1973. Microwave signatures of first year and multi year ice. *J. Geophys. Res.*, 78, C 18, 3564-3572.
Gloersen, P., Campbell, W.J., Cavalieri, D.J., Comiso, J.C., Parkinson, C.L. & Zwally, H.J., 1992. Arctic and Antarctic sea ice, 1978-87: Satellite Passive-Microwave Observations and Analysis. NASA SP-511, NASA Scientific and Technical Information Program, Washington DC, USA, 290 p.
Jeffries, M.O., Li, S., Jana, R.A., Krouse, H.R. & Hurst-Cushing, B., 1998. Late winter first-year ice floe thickness variability, seawater flooding and snow ice formation in the Amundsen and Ross seas. In *Antarctic Sea Ice – Physical Processes, Interactions and Variability*. Antarctic Research Series, American Geophysical Union, vol. 74, pp. 69-87.
Key, J. & Haefliger, M., 1992. Arctic ice surface temperature retrieval from AVHRR thermal channels. *J. Geophys. Res.*, 97, 5885-5893.
Majumdar, T.J. & Mohanty, K.K., 2000. Detection of areal snow cover changes over Antarctica using SSM/I passive microwave data. *Curr. Sci.*, 79, 648-651.

- Maslanik, J. & Key, J., 1993. Comparison and integration of ice-pack temperatures derived from AVHRR and passive microwave imagery. *Annals of Glaciol.*, 17, 372-378.
- Maslanik, J. & Stroeve, J., 2002. DMSP F13 SSM/I Daily Polar Gridded Brightness Temperature: 1990–2002. National Snow and Ice Data Center, Distributed Active Archive Center, University of Colorado at Boulder, Colorado, USA.
- Massom, R., 1991. Satellite Remote Sensing of Polar Regions –Applications, Limitations and Data Availability. Lewis Publishers, Florida, USA, 307 p.
- NSIDC Reports, 1999. 'The DMSP SSM/I Pathfinder daily EASE-Grid brightness temperatures' and 'Sea ice concentrations from Nimbus-7 SMMR and DMSP SSM/I Passive Microwave data'. NSIDC, Colorado, USA. NSIDC Notes, 2008. Antarctic ice shelf disintegration underscores a warming world. NSIDC, Colorado, Issue No. 63, p. 1.
- Sreenivasan, G. & Majumdar, T.J., 2006. Mapping of Antarctic sea ice in the depletion phase: an indicator of climatic change?, *Curr. Sci.*, 19, 851-857.
- Ulaby, F.T., Moore, R.K., & Fung, A.K., 1986. Microwave Remote Sensing: Active and Passive. Artech House, Norwood, 2162 p.
- Zwally, H.J., Comiso, J.C., Parkinson, C.L., Campbell, W.J., Carsey, F.D. & Gloersen, P., 1983. Antarctic Sea Ice, 1973-76: Satellite passive-microwave observations. NASA SP - 459, NASA Scientific and Technical Information Branch, Washington DC, USA, 206 p.



Dr. T. J. Majumdar received Ph. D. in Applied Geophysics from Indian School of Mines, Dhanbad in 1990. Presently working as CSIR Emeritus Scientist and posted at SAC. Formerly Head, Earth Sciences & Hydrology Division, MESG/RESA, Space Applications Centre (ISRO), Ahmedabad. His current fields of interest include satellite geoid/gravity for lithospheric modelling, ASTER data analysis for oil field signatures, satellite data fusion and analysis over Singhbhum Shear Zone for lithological mapping, Antarctic studies using SSM/I passive microwave and Seasat altimeter data, Disaster/earthquake occurrences monitoring using satellite gravity and thermal IR data etc. Dr. Majumdar has around 225 publications/articles in digital image processing and its applications to geophysical remote sensing. Fellow/Life Member, Geological Society of India, Indian Society of Remote Sensing, India Meteorological Society, Indian Society of Geomatics, Indian Society of Earthquake Science.



Mr. S. Bhattacharya received M. Tech. in Applied Geology from Indian Institute of Technology, Kharagpur in 2004. Presently working as a Scientist in Planetary Sciences and Marine Optics Division, MPSP/EPSP, Space Applications Centre (ISRO), Ahmedabad. His current fields of interest include planetary geology with special emphasis to the Moon and the Mars, reflectance spectroscopy, hyperspectral remote sensing for mineral mapping and exploration. He is involved in Chandrayaan-1 data analysis for compositional mapping of the lunar surface. Worked as a visiting scientist at Max-Planck Institute for Solar System Research, Katlenburg-Lindau, Germany on Chandrayaan-1 HySI/SIR-2 and SMART-1 SIR data analyses. Previously he had also worked in the fields of neotectonic activities in the outer Himalaya, Antarctic sea ice mapping, snow and glacier studies. Mr. Bhattacharya has published 10 research papers in peer reviewed national and international journals. Life Member of Indian Society of Remote Sensing, Dehradun.